ELSEVIER

Journal of Molecular Catalysis A: Chemical 170 (2001) 195–202

JOURNAL OF MOLECULAR CATALYSIS A: CHEMICAL

www.elsevier.com/locate/molcata

Acidity enhancement of SBA mesoporous molecular sieve by modification with SO_4^{2-}/ZrO_2

Weiming Hua, Yinghong Yue, Zi Gao*

Department of Chemistry, Fudan University, Shanghai 200433, PR China

Received 19 October 2000; accepted 17 January 2001

Abstract

The SO_4^{2-}/ZrO_2 modified SBA mesoporous molecular sieves were prepared and characterized by XRD, N_2 adsorption, TG/DTG/DTA and IR pyridine chemisorption. The acidity of the molecular sieve was greatly enhanced after modification, and IR pyridine chemisorption results revealed that Lewis acidity was dominant in these samples. The catalytic activities of the modified molecular sieves towards strong and medium strong acid catalyzed reactions were lower than those of bulk SO_4^{2-}/ZrO_2, but higher than those of Al-containing SBA molecular sieve from direct synthesis, whereas the activities of all these catalysts for weak acid catalyzed reaction were close to each other.

Keywords: Acidity; Mesoporous molecular sieve; SBA-15; SO_4^{2-}/ZrO_2

1. Introduction

The newly developed silica mesoporous molecular sieves have attracted increasing interest because of its high surface area, large pore volume and a uniform hexagonal array of cylindrical mesopores [1], which provide the potential for use as catalysts or catalyst supports involving bulky molecules. The silanol groups on the surface of these materials are non-acidic or very weakly acidic, but incorporation of aluminum into the framework of these mesoporous molecular sieves may create new acid sites on the surface [2–10]. However, experimental results reported in the literatures show that the Al-containing materials still have low acidity and low catalytic activity for a number of acid-catalyzed reactions. One reason for that is the incorporation of aluminum through direct synthesis or post-synthesis is limited. The other reason is the inorganic oxide wall of the mesoporous materials is amorphous rather than crystalline as it is in zeolites. Various other modification methods have been employed to enhance the acidity of these new materials, such as sulfating [11], supporting heteropolyacid and SO_4^{2-}/ZrO_2 [12–15], impregnating with iron sulfate [16] and functionalizing with sulfonic acid [17,18]. Nevertheless, most of the works published were focused on the modification of MCM-41 type materials.

The SBA-15 is a newly reported silica mesoporous material prepared by using a triblock copolymer as template [19]. It has a more regular structure and a thicker channel wall than MCM-41, resulting in much higher thermal stability. The material itself is non-acidic like MCM-41. In the present work, we attempted to enhance the acidity of SBA-15 mesoporous molecular sieve by modifying it with SO_4^{2-}/ZrO_2, a well-known strong solid acid. The textural properties as well as acidities of the modified materials were characterized by X-ray diffraction (XRD), N_2 adsorption,

* Corresponding author. Tel.: +86-21-65642792; fax: +86-21-65641740.
E-mail address: zigao@fudan.edu.cn (Z. Gao).

1381-1169/01/$ – see front matter
PII: S1381-1169(01)00063-2

TG/DTG/DTA and IR pyridine chemisorption. Their catalytic activities towards different acid-catalyzed reactions were investigated and compared with those of bulk SO_4^{2-}/ZrO_2 and AlSBA from direct synthesis.

2. Experimental

2.1. Sample preparation

The SBA-15 molecular sieve was prepared as follows [13]: 9 ml of tetraethyl orthosilicate (TEOS) were added to 150 ml of 2 mol l^{-1} HCl solution containing 4 g triblock poly(ethylene oxide)–poly(propylene oxide)–poly(ethylene oxide) (EO_{20}-$PO_{70}EO_{20}$, Aldrich). The mixture was stirred for 3 h at 40°C and allowed to react at 100°C for 48 h. The solid obtained was filtered, dried at 100°C, and finally calcined in air flow at 500°C.

The SO_4^{2-}/ZrO_2 modified samples were prepared as follows. Zirconium nitrate was impregnated onto SBA-15 molecular sieves using an incipient wetness method. The impregnated sample was dried at 110°C and precalcined at 300°C for 3 h. Then, the precalcined sample was treated with 0.5 mol l^{-1} H_2SO_4, filtered, dried at 110°C and calcined at 650°C for 3 h. The final samples were designated as SZ(x)/SBA, where x represented the weight percentages of SO_4^{2-}/ZrO_2 in the samples. AlSBA with Si/Al ratio 10 was prepared according to the literature [8].

2.2. Characterization

X-ray diffraction power data were obtained on a Rigaku D/MAX-IIA diffractometer using Cu Kα radiation at 40 kV and 20 mA. BET surface area, pore volume and pore size distribution were measured under liquid N_2 temperature on a micromeritics ASAP-2000 instrument using N_2 as the adsorbent.

TG/DTG/DTA measurements of the samples were carried out on a Rigaku thermoflex instrument. A 10 mg of sample was heated from room temperature to 900°C at a heating rate of 10°C min^{-1} in flowing N_2.

IR spectra of the samples were recorded on a Perkin-Elmer 983G IR spectrometer. Self-supporting wafers of the samples were evacuated at 400°C for 3 h in the cell at 10^{-4}–10^{-5} Torr and then dosed with an excess of pure pyridine vapor. IR spectra of pyridine chemisorbed were recorded after evacuated at 150–400°C. Bronsted and Lewis acidities were determined on the basis of the absorbance of the PyB band near 1540 cm^{-1} and PyL band near 1450 cm^{-1}.

2.3. Activity tests

The activities of the samples toward cumene cracking and isopropanol dehydration were tested in a pulsed microreactor. The catalyst load for the tests was 50 or 20 mg, respectively, and the catalyst was preheated at 400°C for 3 h in a nitrogen flow before reaction. Hydrogen was used as the carrier gas at a flow rate of 30 and 40 ml min^{-1}. The amount of cumene or isopropanol injected for each test was 1 or 5 μl, respectively. The reaction products were analyzed using a gas chromatograph equipped with a flame ionization detector (FID).

The n-pentane isomerization reaction was carried out at 35°C in a closed reactor system. The catalyst loading was 0.5 g, and the catalyst was evaluated at 250°C for 3 h before reaction. The amount of n-pentane injected for each test was 25 μl. The reaction products were sampled and analyzed by using a gas chromatograph equipped with FID.

3. Results and discussion

3.1. Structural characterization

X-ray diffraction patterns of SBA-15 and SO_4^{2-}/ZrO_2 modified SBA samples after calcination at 650°C are shown in Fig. 1. SBA-15 exhibits one very intense line and two weak lines in the low-angle region, which can be indexed to (1 0 0), (1 1 0) and (2 0 0) diffraction lines characteristic of its hexagonal structure according to the literature [16]. The XRD patterns of SO_4^{2-}/ZrO_2 modified SBA samples give almost the same diffraction peaks as the parent material, indicating that the structure of the mesoporous molecular sieve is intact after modification even with SO_4^{2-}/ZrO_2 content as high as 40 wt.%. In our previous work, it has been observed that MCM-41 loses its mesostructure at a SO_4^{2-}/ZrO_2 loading of 30 wt.% [15], which confirms that SBA-15 is a better support for SO_4^{2-}/ZrO_2 than MCM-41 due to its high stability.

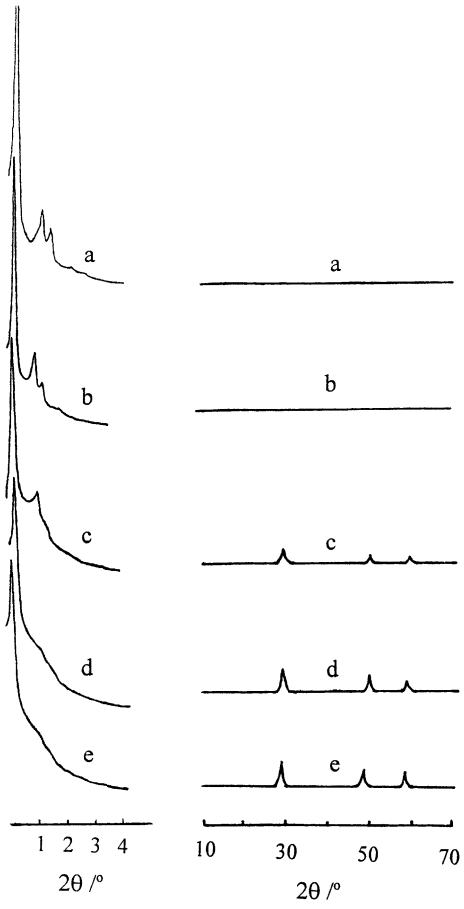

Fig. 1. XRD patterns of the samples calcined at 650°C: (a) SBA-15; (b) SZ(10)/SBA; (c) SZ(20)/SBA; (d) SZ(30)/SBA; (e) SZ(40)/SBA.

No clear XRD peaks are observed in the wide-angle region for the sample with low SO_4^{2-}/ZrO_2 content (10 wt.%), implying that sulfated zirconia is monolayerly or highly dispersed on the surface of the sample. Increasing the SO_4^{2-}/ZrO_2 content to 20 wt.% or above, low and broad peaks that can be index as the (1 1 1), (2 0 2) and (1 3 1) reflections of tetragonal ZrO_2 phase appear on the patterns, indicating that small sulfated zirconia crystallites start to form on the surface of these samples.

Figs. 2 and 3 illustrate the N_2 adsorption/desorption isotherms and pore size distributions of the samples, and their textural properties are listed in Table 1. The isotherm of unmodified SBA sample gives a clear H_1 type hysteresis loop in the relative pressure range between 0.6 and 0.8, suggesting that this material has very regular mesoporous channels. This is also proved by the narrow Gaussian pore size distribution centered at 6.4 nm in Fig. 3a. The N_2 adsorption/desorption isotherms of SO_4^{2-}/ZrO_2 modified samples are similar to that of SBA-15, implying that their mesoporous structure is unchanged after modification, which is in agreement with the above XRD results. Meanwhile, the changes in the pore distributions show that the uniformity of the mesopores decreases with an increase of SO_4^{2-}/ZrO_2 content. A small shoulder peak centered around 4.0 nm appears in the pore size distribution curve of SZ(20)/SBA sample, and it grows larger as the SO_4^{2-}/ZrO_2 content is further increased. The appearance of the peak is related to the fixed closure of the hysteresis loop at a relative pressure close to 0.42 on the N_2 adsorption/desorption isotherm (Fig. 2).

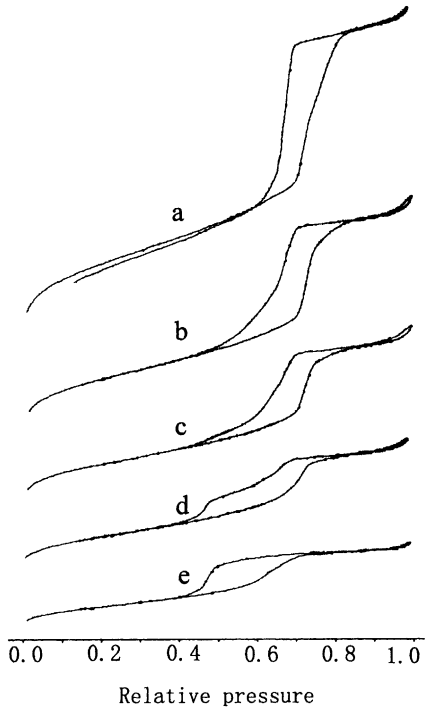

Fig. 2. N_2 adsorption/desorption isotherms of the samples: (a) SBA-15; (b) SZ(10)/SBA; (c) SZ(20)/SBA; (d) SZ(30)/SBA; (e) SZ(40)/SBA.

According to the literature [20], the location of the peak does not represent the true pore size of the sample, but it is characteristic of the adsorptive. Thus, what we can derive from the data is simply

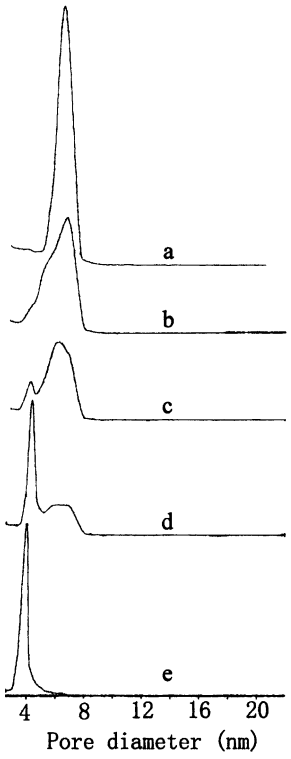

Fig. 3. Pore size distributions of the samples: (a) SBA-15; (b) SZ(10)/SBA; (c) SZ(20)/SBA; (d) SZ(30)/SBA; (e) SZ(40)/SBA.

that non-uniform and finer pores are formed in the samples, and the irregular reduction in pore size is probably caused by blocking of the mesoporous channels with sulfated ZrO_2 crystallites formed at high loading. The BET surface area and pore volume of the samples decrease gradually with SO_4^{2-}/ZrO_2 loading. However, the surface area and pore volumes of SZ(10)/SBA and SZ(20)/SBA samples are still in the range of 380–500 $m^2\,g^{-1}$ and 0.51–0.98 $cm^3\,g^{-1}$, which are sufficient for most catalysts. For comparison, the results of our previous work [15] on MCM-41 and SO_4^{2-}/ZrO_2 modified MCM-41 are listed in Table 1 as well. The surface area and pore volume of the modified MCM-41 sample are smaller than those of the modified SBA sample at the same loading, although the parent MCM-41 has a higher surface area and pore volume than SBA-15, showing that blocking of the mesoporous channels is probably more serious for MCM-41 due to its narrower pore diameter.

TG/DTG/DTA plots of SBA-15, SO_4^{2-}/ZrO_2 and SZ(20)/SBA samples are illustrated in Fig. 4. There is only one endothermic peak at about 50°C for SBA-15 corresponding to desorption of adsorbed water. The weight loss of SBA-15 at 50°C is about 7.2 wt.%, and from 50 to 900°C is about 1.0 wt.%. The latter may correspond to dehydroxylation of silanol groups on the surface. For SO_4^{2-}/ZrO_2 sample, besides the endothermic peak at 57°C, there is an exothermic peak at 791°C corresponding to release of SO_3. The weight losses of SO_4^{2-}/ZrO_2 at dehydration and desulfurization are 2.2 and 3.8 wt.%, respectively. The TG/DTG/DTA profiles of SZ(20)/SBA are almost the same as those of SO_4^{2-}/ZrO_2. Its dehydration and desulfurization occur at 45 and 768°C, respectively. The higher surface area of SZ(20)/SBA (386 $m^2\,g^{-1}$) as compared with SO_4^{2-}/ZrO_2 (113 $m^2\,g^{-1}$) may account for the slight lowering of these temperatures. The weight losses of SZ(20)/SBA, which contains

Table 1
Textural properties of the samples

Sample	BET area ($m^2\,g^{-1}$)	Pore volume ($cm^3\,g^{-1}$)	Pore diameter D (nm)	d_{100}-Spacing (nm)	a_0[a] (nm)	t[b] (nm)	SO_3 (wt.%)
SBA-15[c]	683	0.984	6.4	9.8	11.3	4.9	–
SZ(10)/SBA	505	0.699	6.4	9.8	11.3	4.9	2.4
SZ(20)/SBA	386	0.517	5.8	9.7	11.2	5.4	3.5
SZ(30)/SBA	322	0.384	5.8	9.8	11.3	5.5	3.6
SZ(40)/SBA	208	0.244	–	9.7	–	–	4.8
MCM-41 [15]	1192	1.13	2.8	–	–	–	–
SZ(30)/MCM-41 [15]	307	0.26	2.6	–	–	–	–
SZ	113	–	–	–	–	–	3.8

[a] Unit cell size, $a_0 = 2d_{100}/\sqrt{3}$.
[b] Pore wall thickness, $t = a_0 - D$.
[c] SBA-15 sample calcined at 650°C for 3 h.

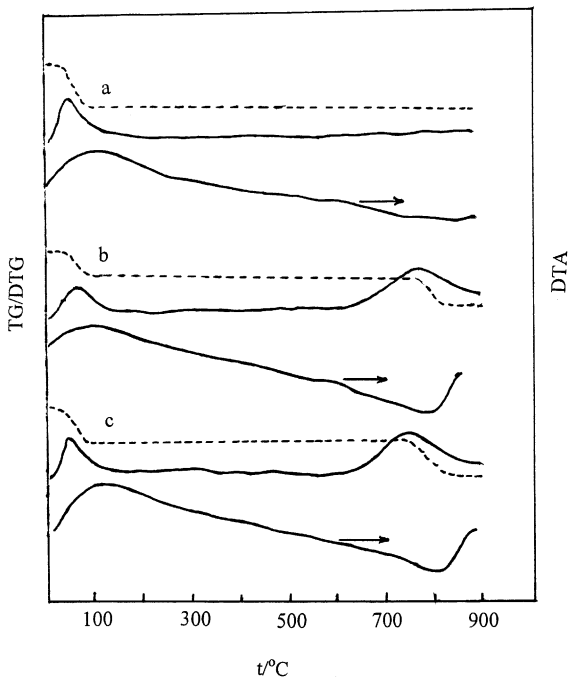

Fig. 4. TG/DTG/DTA plots of the samples: (a) SBA-15; (b) SZ; (c) SZ(20)/SBA.

only 20 wt.% of SO_4^{2-}/ZrO_2, at dehydration and desulfurization are 2.1 and 3.5 wt.%, respectively. The exceedingly high SO_3 content of SZ(20)/SBA arises not only from its high surface area, but also the high dispersion of ZrO_2 on the surface of SBA-15. The SO_3 content of all the other samples determined by TG are listed in Table 1. It has been noted that the SO_3 content does not increase in proportion to the amount of ZrO_2 in the samples, because the surface area and the dispersity of ZrO_2 on the samples decrease with the amount of ZrO_2 added.

3.2. Acidity measurement

Infrared spectra of SBA samples before and after modification with SO_4^{2-}/ZrO_2 were recorded. The adsorption band of asymmetric stretching of S=O double bonds of the surface sulfate complex in SO_4^{2-}/ZrO_2, was commonly found in the adjacency of 1390 cm^{-1} [21]. A small shoulder peak around 1348 cm^{-1} appeared in the spectra of the modified SBA samples. This adsorption band can be assigned to the asymmetric stretch frequency of S=O double bonds of the sulfate complexes in the samples, and the red shift of the frequency may imply a decrease in acid strength of the surface sulfate species due to the strong interaction between SO_4^{2-}/ZrO_2 and SBA support.

The acidities of the samples were measured by IR pyridine adsorption method. The IR spectrum of SBA before pyridine adsorption gave a large and sharp peak at 3740 cm^{-1} corresponding to the presence of a large amount of silanol groups on the surface. After pyridine adsorption at 150°C, an almost unobservable absorption band of very low intensity appeared at 1445 cm^{-1} showing that SBA possesses only a trace amount of Lewis acid sites. Distinct adsorption bands of Bronsted and Lewis acid sites at 1544 and 1445 cm^{-1} were observed in the spectra of SO_4^{2-}/ZrO_2 and SO_4^{2-}/ZrO_2 modified SBA samples. The relative Bronsted and Lewis acidities of these samples were calculated from the adsorbance of PyB band at 1544 cm^{-1} and PyL band at 1445 cm^{-1} and listed in Table 2. It is evident that modification of SBA with SO_4^{2-}/ZrO_2 leads to a substantial increase in its Bronsted and Lewis acidities, and Lewis acidity is dominant in the modified samples. As the evacuation temperature increased, the amount of pyridine adsorbed on the samples decreased. At 400°C, pyridine was only adsorbed on the strong Lewis acid sites of the samples. Tanabe et al. [22] proposed that this strong Lewis acidity is generated by the electron inductive effect of the S=O double bonds in the surface sulfate complex of sulfated zirconia. The authors also suggested that these strong Lewis acid sites may turn into strong Bronsted acid sites after exposure to water or hydrocarbon reactants, so these kind of catalysts are actually active for both Lewis and Bronsted acid catalyzed reactions.

3.3. Catalytic activities

The catalytic behavior of SO_4^{2-}/ZrO_2 modified SBA samples towards different acid catalyzed reactions has been investigated. The *n*-pentane conversion, cumene cracking and isopropanol dehydration have been chosen as strong, medium strong and weak acid catalyzed reactions to test the catalytic activity of these samples.

Table 2
Acidities of the samples measured by IR

Samples	Desorption temperature (°C)	B acidity (10^{-3} a.u. mg cm^{-2})	L acidity (10^{-3} a.u. mg cm^{-2})	Total (10^{-3} a.u. mg cm^{-2})
SZ	150	2.02	53.4	55.4
	300	0.98	23.0	24.0
	400	–	8.57	8.57
SZ(10)/SBA	150	3.53	41.7	45.2
	300	3.20	15.1	18.3
	400	–	5.11	5.11
SZ(20)/SBA	150	2.99	44.4	47.4
	300	1.28	20.6	21.9
	400	–	6.72	6.72

The isomerization of *n*-pentane can proceed at ambient temperature on solid acid catalysts with strong acidity or superacidity, such as SO_4^{2-}/ZrO_2, SO_4^{2-}/TiO_2, SO_4^{2-}/Fe_2O_3 and HM zeolite [23]. SBA-15, AlSBA and SZ(10)/SBA samples are not catalytically active for *n*-pentane reaction at 35–75°C, implying that these samples do not have the strong acidity which is essential for the reaction. The *n*-pentane is isomerized on SZ(20)/SBA at 35°C. The major reaction products are isobutane and isopentane, and the selectivity to isopentane decreases with an increase in conversion (see Table 3). The activity of SZ(20)/SBA is lower than that of SO_4^{2-}/ZrO_2 ($H_0 = -16.0$) and SO_4^{2-}/Fe_2O_3 ($H_0 = -13$), but higher than that of HM zeolite ($H_0 = -12.4$) [23], so the acid strength of SZ(20)/SBA is probably in the range of $H_0 = -12.4$ to -13.0, which is much lower than that of bulk SO_4^{2-}/ZrO_2 but still higher than 100% H_2SO_4 ($H_0 = -12$).

The catalytic activities of the samples for cumene cracking and isopropanol dehydration are given in Tables 4 and 5. SBA-15 molecular sieve is inactive for cumene cracking and its activity for isopropanol dehydration is very low, because the silanol groups on its surface are non-acidic or very weakly acidic. The activities of the other catalysts for cumene cracking

Table 3
The *n*-pentane isomerization activity at 35°C

Sample	Reaction time (h)	Conversion (%)	Product distribution (mol%)			*i*-C_5 selectivity (%)
			i-C_4	*i*-C_5	*n*-C_5	
SZ(20)/SBA	5.5	1.4	–	1.4	98.6	100
	11.5	2.3	1.1	1.3	97.6	61
	17.5	4.0	2.5	1.9	95.6	48
	36.0	6.5	3.9	3.3	92.8	51
	58.5	9.2	6.3	4.1	89.6	45
SZ [23]	1.0	25.2	–	25.2	74.8	100
	1.3	40.8	0.1	40.7	59.2	100
	1.7	51.0	0.1	50.9	49.0	100
SO_4^{2-}/Fe_2O_3 [23]	0.5	3.4	1.0	2.4	96.6	75
	1.0	5.8	1.7	4.1	94.2	75
	1.5	6.1	1.6	4.5	93.9	78
HM [23]	66.0	4.7	–	4.7	95.3	100
	84.0	6.7	–	6.7	93.3	100
	108.5	8.7	–	8.7	91.3	100

Table 4
Cumene cracking activities of the samples

Samples	Conversion (%)		
	200°C	250°C	300°C
SBA-15	0	0	0
SZ(10)/SBA	7.0	8.8	14.2
SZ(20)/SBA	29.1	41.8	62.8
SZ	–	61.3	83.4
AlSBA(10)	2.5	15.0	38.2

Table 5
Isopropanol dehydration activities of the samples

Samples	Conversion (%)		
	150°C	200°C	250°C
SBA-15	0	1.6	7.4
SZ(10)/SBA	0.8	17.0	63.5
SZ(20)/SBA	28.8	68.3	100
SZ	27.0	70.0	99.1
AlSBA(10)	23.2	64.0	93.0

are in the order of SZ > SZ(20)/SBA > AlSBA > SZ(10)/SBA, which is consistent with results of IR pyridine adsorption measurements. For isopropanol dehydration, the activities of the catalysts are in the order of SZ ≈ SZ(20)/SBA, AlSBA > SZ(10)/SBA > SBA, which is in agreement with results of sulfate content detected by TG. The differences in the performance of the SO_4^{2-}/ZrO_2 modified catalysts toward the three different acid catalyzed reactions confirm that the total number of acid sites on the surface of SZ(20)/SBA is probably close to that of pure SZ due to the high surface area of SBA-15 and the high dispersion of sulfated zirconia on its surface, but the acid strength of the acid sites is lowered due to the strong interaction between ZrO_2 and the silica mesoporous molecular sieve. Hence, the modified catalysts are probably more suitable for medium strong and weak acid catalyzed reactions.

4. Conclusion

The low acidity and catalytic activity of SBA-15 mesoporous molecular sieve towards acid-catalyzed reactions can be enhanced effectively by modification with SO_4^{2-}/ZrO_2. The mesoporous structure of SBA-15 is intact after modification. The sulfate content of SZ(20)/SBA is close to that of pure SO_4^{2-}/ZrO_2, because of the high surface area of SBA-15 and the high dispersion of SO_4^{2-}/ZrO_2 on its surface. Both Bronsted and Lewis acid sites are formed on the catalysts after modification, but Lewis acid sites are dominant. The catalytic activities of SZ(20)/SBA for strong and medium strong acid catalyzed reactions are lower than those of bulk SO_4^{2-}/ZrO_2, but higher than those of AlSBA from direct synthesis, whereas its activity towards weak acid catalyzed reaction is close to those of the other two catalysts.

Acknowledgements

This work is supported by the Major State Basic Research Development Program (Grant No. 2000077500) and the Foundation for University Key Teachers by the Ministry of Education.

References

[1] C.T. Kresge, M.E. Leonowicz, W.J. Roth, J.C. Vartuli, J.S. Beck, Nature 359 (1992) 710.
[2] R. Schmidt, D. Akporiaye, M. Stocker, O.H. Ellestad, J. Chem. Soc. Chem. Commun. (1994) 1493.
[3] Z.H. Luan, C.F. Cheng, W.Z. Zhou, J. Klinowski, J. Phys. Chem. 99 (1995) 1018.
[4] K.R. Kloetstra, H.W. Zandbergen, H. van Bekkum, Catal. Lett. 33 (1995) 157.
[5] R.B. Borade, A. Clearfield, Catal. Lett. 31 (1995) 267.
[6] J.M. Kim, J.H. Kwak, S. Jun, R. Ryoo, J. Phys. Chem. 99 (1995) 16742.
[7] Y. Sun, Y.H. Yue, Z. Gao, Appl. Catal.: Gen. A 161 (1997) 121.
[8] S. Gontier, A. Tuel, Stud. Surf. Sci. Catal. 101 (1997) 29.
[9] Y.H. Yue, A. Gédéon, J.-L. Bonardet, J.B. D'Espinose, N. Melosh, J. Fraissard, Chem. Commun. (1999) 1967.
[10] R. Mokaya, W. Jones, Chem. Commun. (1997) 2185.
[11] L.W. Chen, C.Y. Chou, A.N. Ko, Appl. Catal. A 178 (1999) L1.
[12] I.V. Kozhevnikov, A. Sinnema, R.J.J. Jansen, K. Pamin, H. van Bekkum, Catal. Lett. 30 (1995) 241.
[13] W. Chu, X. Yang, Y. Shan, X. Ye, Y. Wu, Catal. Lett. 42 (1996) 201.
[14] Y. Sun, Y. Yue, H. Li, Z. Gao, Acta Chim. Sinica 57 (1999) 746.
[15] T. Lei, W.M. Hua, Y. Tang, Y.H. Yue, Z. Gao, Chem. J. Chin. Univ. 21 (2000) 1240.

[16] J.K.A. Dapaah, Y. Uemichi, A. Ayame, H. Matsuhashi, M. Sugioka, Appl. Catal. A 187 (1999) 107.
[17] W.M. Van Rhijn, D.E. Devas, B.F. Sels, W.D. Bassaert, P.A. Jacobs, Chem. Commun. (1998) 317.
[18] M.H. Lim, C.F. Blanford, A. Stein, Chem. Mater. 10 (1998) 467.
[19] D. Zhao, J. Feng, Q. Huo, N. Melossh, G.H. Fredrickson, B.F. Chmelka, G.D. Stucky, Science 279 (1998) 548.
[20] S.J. Gregg, K.S.W. Swing, Adsorption, Surface Area and Porosity, Academic Press, London, 1982.
[21] T. Yamaguchi, T. Jin, K. Tanabe, J. Phys. Chem. 90 (1986) 3148.
[22] K. Tanabe, H. Hattori, T. Yamaguchi, Crit. Rev. Surf. Chem. 1 (1990) 1.
[23] Z. Gao, J.M. Chen, W.H. Hua, Y. Tang, Stud. Surf. Sci. Catal. 90 (1994) 507.